

# Analytical Method of Torque Calculation for Interior Permanent Magnet Synchronous Machines

Seong Taek Lee<sup>1</sup>

Student Member, IEEE

<sup>1</sup>University of Tennessee  
414 Ferris Hall  
Knoxville, TN 37996, USA  
slee10@utk.edu

Leon M. Tolbert<sup>1,2</sup>

Senior Member, IEEE

<sup>2</sup>Oak Ridge National Laboratory  
2360 Cherahala Boulevard  
Knoxville, TN 37932, USA  
tolbert@utk.edu

*\*Abstract -- This paper introduces a new analytical method for performing the output torque calculations of an interior permanent magnet synchronous motor (IPMSM) including both permanent magnet and reluctance torque components. This method works well when using a 2-dimensional magnetic equivalent circuit of a machine by omitting the step of calculating the inductance values which are required for the calculation of the reluctance torque. The analysis results show that this method is very useful in the first design step before simulating a model using finite elements analysis (FEA). Also, this method can be applied to any type of synchronous machine.*

**Index Terms**— equivalent circuit, inductance, permanent magnet machine, synchronous motors, torque.

## I. NOMENCLATURE

BFE	brushless field excitation
IPMSM	interior permanent magnet synchronous motor
FEA	finite element analysis
mmf	magnetomotive force
PM	permanent magnet

## II. INTRODUCTION

The interior permanent magnet synchronous motor (IPMSM) is currently used in many industrial areas due to its advantages of high power density and efficiency. In the first step of designing a new IPMSM, the magnetic equivalent circuit is widely used by many machine designers to determine the characteristic of the machine [1]–[7].

Since the output torque of an IPMSM contains the reluctance torque that is caused by the difference of the two-axes (d- and q-axis) inductances,  $L_d$  and  $L_q$ , these inductance values should be calculated from the analysis of its equivalent circuit. In other words, to obtain the output torque of a newly designed machine, the exact inductance values ( $L_d$  and  $L_q$ ) are necessary [1], [3]–[5], and [7]–[9]. There are many analytical methods to calculate the  $L_d$  and  $L_q$  of synchronous motors including IPMSM [1], [3], [4], and [10]–[11]. However, it is not easy to calculate the  $L_d$  and  $L_q$ , because these inductance

values are dependent on the applied current value. Also, the present method of calculating the reluctance torque is performed under the assumption that all load current and the magnetic flux flow only along the two-axes.

This paper presents a new analytical method of calculating the output torque of an IPMSM using a 2-dimensional magnetic equivalent circuit, without the step of calculating the inductance values by considering the actual distribution of the load current and flux. The results will be compared to the results of Finite Element Analysis and experimental test.

## III. TORQUE EQUATION OF IPMSM

Below is the well-known electromagnetic torque equation of all synchronous machines based on the conventional two-axes machine model [3]–[11]:

$$T = \frac{m}{2} p (\lambda_d i_q - \lambda_q i_d) \quad (1)$$

In (1),  $m$  is the number of phase conductors,  $p$  is the number of pole pairs,  $\lambda$  is the flux linkage, and  $i$  is the instantaneous current. The subscripts  $d$  and  $q$  indicate the d-axis and q-axis, respectively. In the case of the classical analysis, the flux linkage has the following mathematical relationship;

$$\begin{aligned} \lambda_d(i_d) &= \lambda_{d,PM} + L_d i_d \\ \lambda_q(i_q) &= L_q i_q \end{aligned} \quad (2)$$

where the term  $\lambda_{d,PM}$  is the d-axis flux linkage from the rotor flux (usually from permanent magnets). Substituting the terms from (2) into (1), the conventional torque equation of IPMSM becomes

$$T = \frac{m}{2} p (\lambda_{d,PM} i_q + (L_d - L_q) i_d i_q) \quad (3)$$

The first term in (3) is called permanent magnet torque and the second is reluctance torque. Equation (3) shows that the values of  $\lambda_{d,PM}$ ,  $L_d$ , and  $L_q$  are necessary to obtain the output torque. These values are usually calculated by the analysis of the equivalent circuit. Equation (3) also assumes that all the

\*The submitted manuscript has been authored by a contractor of the U. S. Government under contract no. DE-AC05-00OR22725. Accordingly, the U.S. Government retains a nonexclusive, royalty-free license to publish or reproduce the published form of this contribution, or allow others to do so, for U. S. Government purposes. Research sponsored by the Oak Ridge National Laboratory managed by UT-Battelle, LLC for the U. S. Department of Energy under contract DE-AC05-00OR22725.

load current and magnetic flux flow only along the two-axes respectively.

#### IV. NEW METHODOLOGY OF OUTPUT TORQUE CALCULATION

In a conventional method using an equivalent circuit, the output torque calculation has several steps: 1) calculate the PM torque, 2) calculate d-axis inductances, 3) calculate q-axis inductance, 4) estimate the reluctance torque, 5) add the PM and reluctance torque [1], [4]–[6], and [8]–[9].

The above conventional method is not simple and is based on the fundamental component of the air-gap flux. Moreover, the present method of calculating the reluctance torque is under the assumption that all mmf from phase current and the magnetic flux flow to only the two-axes (d- and q- axes) in the machine.

The new method can obtain the reluctance and total output torque characteristics with one step by considering the actual distribution of the load current and magnetic flux in a 2-dimensional magnetic equivalent circuit. In other words, this method enables omission of the step of calculating the values of  $\lambda_{d,PM}$ ,  $L_d$ , and  $L_q$  by using nodal analysis of the 2-dimensional equivalent circuit.

The base concept is simple; the total output torque should be the cross product between the current at the stator coils and the flux linkage caused from the rotor. Fig. 1 is the conceptual equivalent circuit of an IPMSM, which has  $4n$  column rods at the stator and rotor respectively over 1 pole-period. The column rods at stator and rotor are connected by an air-gap reluctance network to each other, and there are mmf sources at the stator part, which are modeled for the phase current. The values of the mmf sources are determined by the current density at the stator.  $\Phi_k$  is the air-gap flux at the  $k_{th}$  rod of the air-gap determined by the applied current at the stator.

Because (1) suggests that the output torque is determined by the cross-product between the flux linkage and the applied current with the electrical angle difference of  $90^\circ$ , the new torque equation applied to this equivalent circuit is

$$T = \frac{p}{2} \left[ \begin{aligned} & (\lambda_{n+1}i_1 - \lambda_1i_{n+1}) + (\lambda_{n+2}i_2 - \lambda_2i_{n+2}) + \\ & \dots + (\lambda_{4n}i_{3n} - \lambda_{3n}i_{4n}) \\ & + (\lambda_1i_{3n+1} - \lambda_{3n+1}i_1) + (\lambda_2i_{3n+2} - \lambda_{3n+2}i_2) + \\ & \dots + (\lambda_ni_{4n} - \lambda_{4n}i_n) \end{aligned} \right] = \frac{p}{2} \left[ \sum_{k=1}^{3n} (\lambda_{n+k}i_k - \lambda_ki_{n+k}) + \sum_{k=1}^n (\lambda_ki_{3n+k} - \lambda_{3n+k}i_k) \right] \quad (4)$$

where  $\lambda_k$  is the flux linkage caused by  $\Phi_k$ . If the machine is symmetric between the d and -d axes, the torque equation (4) can be simplified to

$$T = p \sum_{k=1}^{2n} (\lambda_{n+k}i_k - \lambda_ki_{n+k}) \quad (5)$$

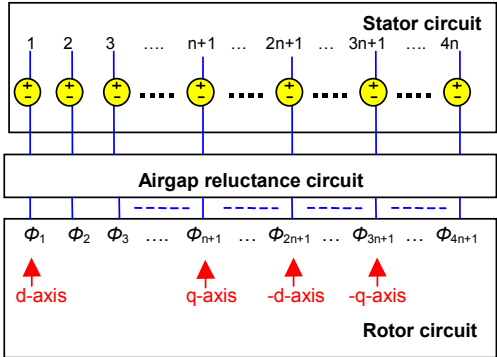


Fig. 1. Conceptual 2D-equivalent circuit of an IPMSM.

#### V. VERIFYING NEW METHOD

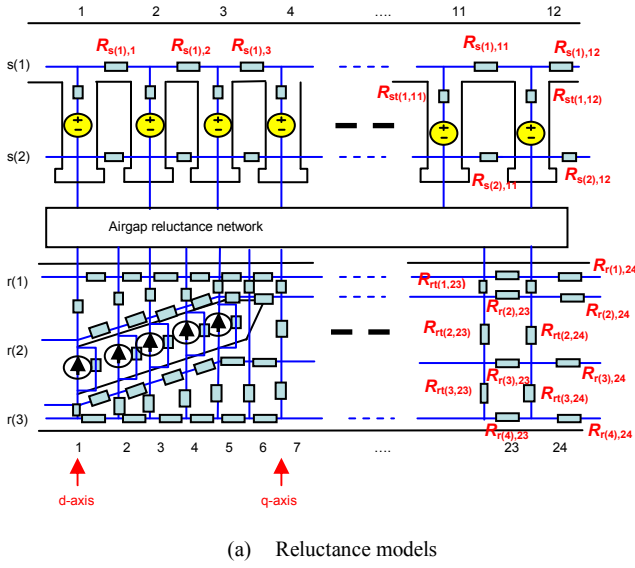
##### A. Prius IPMSM

Fig. 2 (a) is the equivalent circuit of the 2004 Toyota Prius IPMSM used for this analysis. This circuit has 2 row and 12 column rods at the stator part and 4 row and 24 column rods at the rotor part. Every node at the stator part is indicated as  $s(i,j)$  that means the node intersecting between the row  $s(i)$  and column  $j$  at the stator. Similarly, at the rotor part each node is named as  $r(i,j)$  between the row  $r(i)$  and column  $j$ . The last column node  $s(1,12)$  is connected to the node  $s(1,1)$  and  $r(1,24)$  to  $r(1,1)$  because the machine is periodic with the repeated North and South poles.

Every stator node  $s(2,i)$  is connected to all nodes on the row  $r(1)$  of the rotor,  $r(1,1)$  through  $r(1,24)$ . Fig. 2 (b) is a sample illustration showing how the air-gap reluctances from stator node  $s(2,1)$  is connected to every rotor node on the row  $r(1)$ .

There are independent mmf sources at each stator node caused by the phase current, and the value of each mmf source is changed to meet input current value and load angle. The independent flux sources in the rotor part are from the modeling of the permanent magnets inside the rotor.

Applying the nodal analysis method to the equivalent circuit based on Kirchoff's current law, the nodal potential at every node in the equivalent circuit can be calculated, and then the flux linkage from each node of the first row at the rotor can also be obtained. The detailed process of solving the equivalent circuit is presented in [14].



(a) Reluctance models

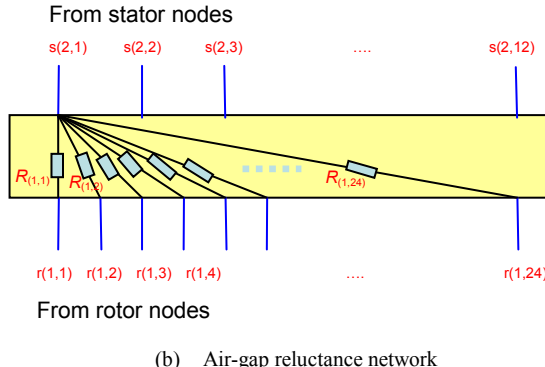


Fig. 2. 2D-equivalent circuit of Prius IPMSM.

Since this Prius model is symmetric between the d and  $-d$  axes and the circuit has 12 column rods at the stator and 24 rods at the rotor, the torque equation (5) can be simplified to (6).

$$T = 4 \sum_{k=1}^6 (\lambda_{(2k+5)} i_{(k)} - \lambda_{(2k-1)} i_{(k+3)}) \quad (6)$$

Fig. 3 is the output torque graph obtained from (6), which is compared with the FEA and experimental test results. The graphs show that the overall analysis results agree with the experimental test results. Fig. 4 is the expected reluctance torque graph that is calculated with no-magnetized permanent magnets in the rotor by equivalent circuit (the value of all flux sources is zero) and FEA simulation. Fig. 4 proves that the new method of the output torque calculation will be very effective in designing a new IPMSM if a machine designer tries to increase the reluctance torque because the new method has simpler process to determine the reluctance

torque profiles along with the input current. It is not necessary to analyze d- and q- axis inductance values for every rotor dimension in draft designs by using the equivalent circuit approach.

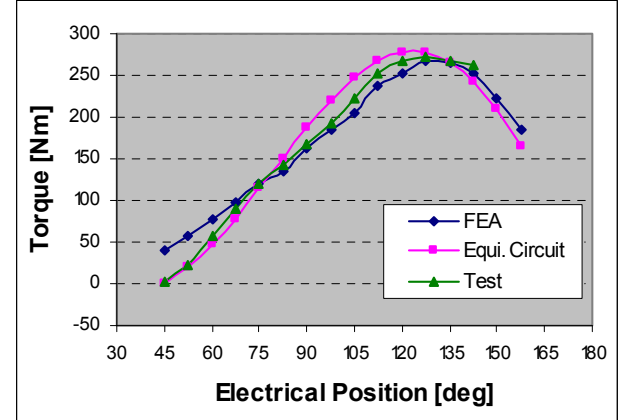


Fig. 3. Output torque @ 150 A load current.

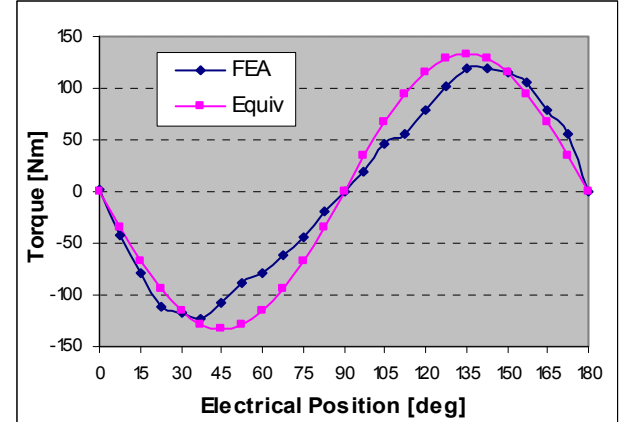


Fig. 4. Expected reluctance torque @ 150A load current.

#### B. IPMSM with slanted air-gap

This new method is more effective when the machine has non-uniform air-gap such as slanted air-gap structure shown in Fig. 5. This structure is for increasing its output torque and the controllable back emf ratio which is enabled by the structure of the brushless field excitation that produce axial flux. This flux is added to the main flux from the PMs inside the rotor and interacts with the stator current to produce motor torque. The details are presented in [12]–[14].

The assembled prototype of the Oak Ridge National Laboratory (ORNL) 16,000-rpm motor design is shown in Fig. 6. Table I compares the dimensions of the ORNL 16,000-rpm motor with those of a Toyota Prius motor that was selected as a baseline motor.



Fig. 5 Assembled rotor core stack.

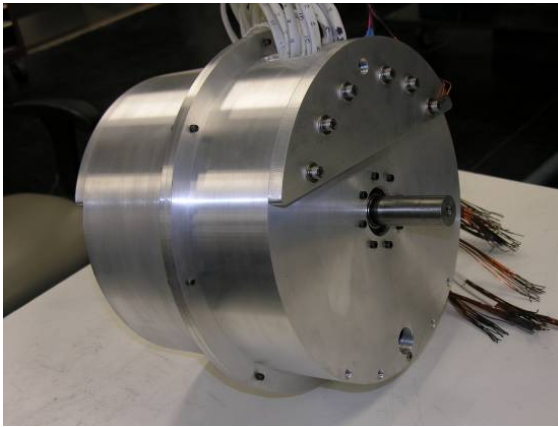


Fig. 6. Assembly of ORNL 16,000-rpm motor.

TABLE I  
Comparison of Dimensions of the ORNL 16,000-rpm Motor and the Baseline Motor

	<b>Prius</b>	<b>ORNL</b>
Speed	6,000 rpm	16,000 rpm
Stator lamination outer diameter	269.2 mm	269.2 mm
Rotor outer diameter	160 mm	160 mm
Core length	83.82 mm	47.75 mm
Bearing to bearing outer face	196.85 mm	189.23 mm
Magnet weight	1.25 kg	1.16 kg
Estimated field adj. ratio	none	2.5
Rating	33/50 kW	33/50 kW
Boost converter	yes	no
High-speed core loss	high	low

The prototype has its slanted air-gap in 2.54 mm (0.1 inches) of the maximum depth and a half span width between two vertical PMs inside the rotor. These dimensions are determined after investigating various slanted air-gap shapes using the new output torque calculation method.

Because of its slanted air-gap shape, the reluctance torque position will be shifted from 135° toward 90° to increase its total output torque (PM torque + reluctance torque). In a conventional method of using an equivalent circuit, it is impossible to calculate the shift angle of the reluctance torque caused by the slanted air-gap shape. However, by using the new method, the expected reluctance torque profile can be obtained easily. The details of construction and solving process of the equivalent circuit of the ORNL 16,000-rpm motor are presented in [14].

Fig. 7 is the expected reluctance torque graphs of the prototype IPMSM, which are obtained from the equivalent circuit and FEA analyses. This graph clearly shows that the maximum reluctance torque position is 105° not 135°. Similarly, the maximum output torque position is also shifted toward 90 ° as shown in Fig. 8 and Fig. 9.

Fig. 8 is the comparison of total output torque when the maximum input current is 200 A in comparison of analysis results and experimental test results. Fig. 9 is the comparison for the case of the maximum input current is 50 A. The overall results from the equivalent circuit are agreeable with the experimental test results.

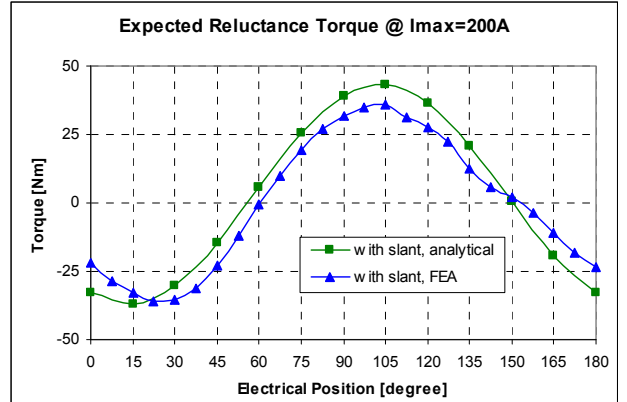


Fig. 7. Comparison of the expected reluctance torque.

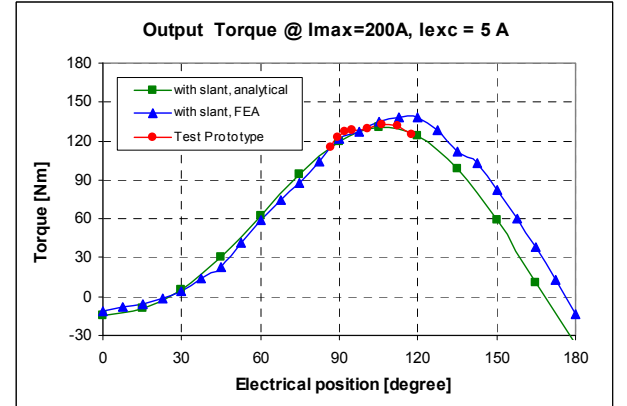


Fig. 8. Comparison of the expected output torque at  $I_{max}=200A$ .

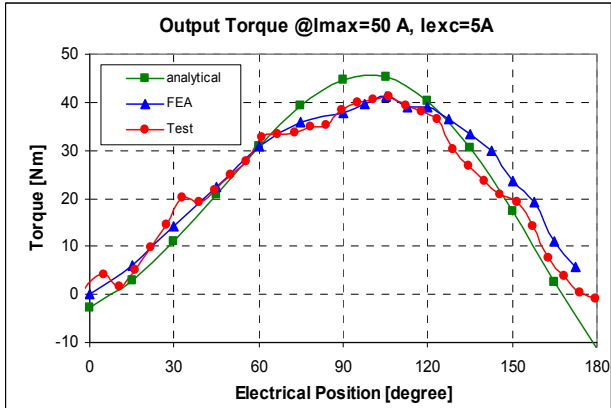


Fig. 9. Comparison of the expected output torque at  $I_{max}=50A$ .

## VI. CONCLUSIONS

The possibility of the direct calculation of the expected reluctance torque is a major advantage in new output torque calculation method, because a conventional method needs the values of  $L_d$  and  $L_q$  for calculating reluctance torque for every dimensional change of the machine structure. Therefore, this new output torque calculation method is very useful for designing a new machine especially at the beginning step. Moreover, this method is more effective if the machine has non-symmetrical air-gap shape for shifting its reluctance torque position. Increasing the number of the nodes in the equivalent circuit will produce output torque curves that more closely follow the experimental results.

## REFERENCES

- [1] T. J. E. Miller, *Brushless Permanent-Magnet and Reluctance Motor Drive*, Clarendon Press, U. K. 1989.
- [2] D. C. Hanselman, *Brushless Permanent-Magnet Motor Design*, McGraw-Hill, Inc, U.S. 1994.
- [3] I. Boldea, *Reluctance Synchronous Machines and Drives*, Oxford University Press, U.S. 1996.
- [4] E. C. Lovelace, T. M. Jahns, and J. H. Lang, "A Saturating Lumped-Parameter Model for an Interior PM Synchronous Machine," *IEEE Transactions on Industry Applications*, Jun. 2002, vol. 38, no. 3, pp. 645 – 650.
- [5] E. C. Lovelace, T. Kelim, J. H. Lang, D. D. Wentzloff, T. M. Jahns, J. Wai, and P. J. McCleer, "Design and Experimental Verification of a Direct-Drive Interior PM Synchronous Machine Using a Saturable Lumped-Parameter Model," *IEEE Industry Applications Society Annual Meeting*, Oct. 2002, vol. 4, pp. 2486 – 2492.
- [6] J. Farooq, S. Srairi, A. Djerdir, and A. Miraoui, "Use of Permeance Network Method in the Demagnetization Phenomenon Modeling in a Permanent Magnet Motor," *IEEE Transactions on Magnetics*, Apr. 2006, vol. 42, no. 4, pp. 1295 – 1298.
- [7] S. A. Nasar, I. Boldea, and L. E. Unnewehr, *Permanent Magnet, Reluctance, and Self-Synchronous Motors*, CRC Press Inc, U.S. 1993.
- [8] F. Libert and J. Soulard, "Design Study of Different Direct-Driven Permanent-Magnet Motors for a Low Speed Application," *Proceeding of the Nordic Workshop on Power and Industrial Electronics*, Norway, Jun. 2004.
- [9] S-I. Kim, G-H. Lee, J-P. Hong, and T-U. Jung, "Design Process of Interior PM Synchronous Motor for 42-V Electric Air-Conditioner System in Hybrid Electric Vehicle," *IEEE Transactions on Magnetics*, Jun. 2008, vol. 44, no. 6, pp. 1590 – 1593.
- [10] Y. K. Chin and J. Soulard, "Design Study of a Traction Motor for Electric Vehicle," *Proceeding of the International Conference on Electrical Machines and Systems*, Sep. 2005, vol. 1, pp. 786 – 791.
- [11] K. Alitouche, R. Saou, and M. E. Zaim, "Analytical Optimization of Inset Permanent Magnets Machine Based on a Genetic Algorithm," *International Aigan Conference on Electrical Machines and Power Electronics*, Sep. 2007, pp. 440 – 445.
- [12] J. S. Hsu, S. T. Lee, R. H. Wiles, C. L. Coomer, K. T. Lowe, and T. A. Burriss, "Effect of Side Permanent Magnets for Reluctance Interior Permanent Magnet Machines," *IEEE Power Electronics Specialists Conference*, Jun. 2007, pp. 2267 – 2272.
- [13] J. S. Hsu, T. A. Burriss, S. T. Lee, R. H. Wiles, C. L. Coomer, J.W. McKeever, and D. J. Adams, "16,000-RPM Interior Permanent Magnet Reluctance Machine with Brushless Field Excitation," *IEEE Industry Applications Society Annual Meeting*, Oct. 2008, pp. 1 – 6.
- [14] S. T. Lee, "Development and Analysis of Interior Permanent Magnet Synchronous Motor with Field Excitation Structure," Ph. D. dissertation, Dept. Elec. Eng., Univ. Tennessee, Knoxville, 2009.